Study of the microstructure of durum wheat endosperm using X-ray micro-computed tomography

Lydie Besançon, Eric Rondet, Joël Grabulos, Valerie V. Lullien-Pellerin, Leslie Lhomond, Bernard Cuq

Study of the microstructure of durum wheat endosperm using X-ray micro-computed tomography

Lydie Besançon[a], Eric Rondet[b], Joël Grabulos[b],
Valérie Lullien-Pellerin[a], Leslie Lhomond[c], Bernard Cuq[a *]

[a] UMR IATE, INRAE, l'Institut Agro - Montpellier SupAgro, Université de Montpellier, Montpellier, France.

[b] UMR QualiSud, Université de Montpellier, CIRAD, l'Institut Agro - Montpellier SupAgro, Université d'Avignon, Université de La Réunion, Montpellier, France.

[c] Comité Français de la Semoulerie Industrielle (CFSI), Paris, France.

***Corresponding author :**

Bernard CUQ, Professor,

UMR IATE, l'Institut Agro Montpellier - SupAgro, 2 Place Pierre Viala, 34060, Montpellier, France.

Email : bernard.cuq@supagro.fr

Tel : +33(0)499612860

ABSTRACT

Durum wheat grains are used for producing food, such as pasta or couscous. The grain mechanical properties which are linked to its internal micro-structure (i.e. endosperm porosity) are known to determine its ability to produce semolina during milling. The proportion of grains having porous endosperm in a batch appears therefore as a critical quality factor for the durum wheat value chain. Our objective was to investigate the ability of X-ray micro-tomography (µCT) method to describe the porous or vitreous counterpart structures in the endosperm of durum wheat grains. We selected two different durum wheat samples displaying vitreous or partially porous endosperms. The grains were analyzed using µCT at two pixel sizes (1 µm or 7 µm). The µCT data collected at 7 µm pixel size were used for qualitative classification of grains according to apparent distribution curve of the porosity parameters. Analysis of µCT images at 1 µm pixel size allowed us to propose pore size classification in the vitreous and porous parts of the endosperm in three durum wheat grain. Results are used to better describe the durum-wheat endosperm microstructure, but requires long scanning periods.

Keywords: durum wheat grains, X-ray micro-tomography, endosperm structure, porosity.

1. Introduction

Durum wheat grains are used for producing traditional food, such as pasta or couscous. Controlling the quality of grains is a major challenge for the sustainability of the durum wheat chain. Grains characteristics impact their behavior during the milling stage, with the objective to recover a maximum yield of high quality semolina (Sissons et al., 2012). Milling of durum wheat grains with porous endosperm results in lower semolina yield. Therefore, proportion of grains with porous or vitreous endosperm in a batch is a critical quality factor for the durum wheat chain (Raggiri et al., 2014).

Several characteristics of durum wheat grains can be related to their milling behavior. Hardness measurements describe their mechanical resistance and varies according to vitreousness. Vitreousness is a visual property of the endosperm which is due to a lack of air spaces inside the structure. Vitreous grain has a glassy and translucent appearance, whereas porous endosperm displays a white aspect. The formation of porous structures in durum wheat grains depends on varietal specificities, agronomic stresses, and protein content (Dexter et al., 1989; Samson et al., 2005; Fu et al., 2018). Significant differences in density have been revealed between vitreous and porous endosperms (Samson et al., 2005). An increase in the endosperm porosity appears to lower the semolina yield upon milling.

Description of the endosperm porosity of durum wheat grains has been considered using several specific analytical methods. For instance, the Pohl grain cutter method is a reference method based on cutting a large number of grains and determining by visual inspection the percentage of grains displaying a porous aspect at the cut surface (AFNOR, 2014). This method does not determine the respective volumes of vitreous part and porous parts in the grain endosperm but examines only the half height cut surface. The single kernel characterization system (SKCS) method measures the mechanical resistance of single grains allowing the evaluation of the sample's mean crush force. The SKCS value was shown to be related to the vitreousness value of the durum wheat grain sample (Sissons et al., 2000). Different methods based on image analysis of durum wheat kernels under specific illumination conditions by reflection or transmission have also been used to classify durum wheat grains according to their vitreousness. Near infrared imaging techniques have been tested for discriminating vitreous and porous wheat grains (Vermeulen et al., 2018). Vitreous wheat grains present higher light transmission coefficients than grains displaying partly porous endosperm (Chichti et al., 2018; Edwards et al., 2005; Venora et al., 2009). Kaya and Saritas (2019) described vitreousness of durum wheat grains based on analysis of grain morphology, color, and texture features based on an image acquisition system.

Methods using imaging systems based on real time soft X-rays have been investigated for classifying durum wheat grains (Neethirajan et al., 2007; Neethirajan et al., 2006). X-ray 2D images were used at low resolution (17 µm) for classifying vitreous and porous kernels in durum wheat by using artificial neural networks. X-ray microtomography (µCT) techniques have been able to characterize internal structure of different cereal grains. Endosperm structure of rice kernels was described with a high-resolution µCT at 4 µm pixel size (Zhu et al., 2012). Wild rice grains displayed tightly packed endosperm and little air space, while high amylose rice grains contained numerous air spaces. µCT images were explored to investigate the changes in endosperm structure of wheat grains as function of genotype and development stages under ~~in~~ different growth conditions (Le et al., 2019; Strange et al., 2015). µCT methods allowed the evaluation of the physical damage of the wheat grains upon insect or fungal infestation (Suresh and Neethirajan, 2015) and the impacts of roasting process on the microstructure of whole wheat grains (Schoeman et al., 2016).

The objective of the present study was to investigate the ability of µCT method to describe the vitreous or porous structures in durum wheat grains endosperm. Two different durum wheat samples displaying either vitreous or partially porous endosperms were selected. Grains were analyzed using µCT at two pixel sizes (1 µm or 7 µm). The µCT data collected at 7 µm pixel size were used for qualitative classification and discrimination of grains according to the apparent distribution curve of the porosity parameters. Analysis of µCT images at 1 µm pixel size allowed to describe the microstructure of the vitreous and porous parts in of the durum wheat grain endosperm.

2. Materials and methods

2.1. Raw materials

Durum wheat grains from two different varieties (Karur, Pescadou) were kindly given by Arvalis (Institut du Végétal, France). The grains were cleaned to remove broken kernels and randomly sampled before analysis. The water content (12.4 (± 0.2) and 12.8 (± 0.2) % humid matter, respectively) and the protein content (12.4 (± 0.4) and 15.5 (± 0.4) g proteins / 100 g dry matter, respectively) were determined by Near-Infrared Spectroscopy using the ICC recommendation N°202 (ICC, 1986) with French standards NF V03-707 (AFNOR, 2010) and NF V03-767-2 (AFNOR, 2016) calibration. Grains vitreousness was measured using a Pohl grain cutter which roughly cut the grain in the middle (AFNOR, 2014). The proportion of grains displaying a porous aspect at the cut surface was determined three times in-50 grains. Grains were classified as vitreous when the cut surface is fully translucent/glassy whereas they were classified as porous when at least one mealy area appears on the cut surface. Grains of Pescadou variety were fully vitreous (0% of porous grains) and those of Karur variety were partially porous (33 (±3) % of porous grains).

2.2. X-ray micro-computed tomography acquisition

The endosperm structure of intact durum wheat grains was analyzed using the Skyscan 1272 X-ray micro-tomograph (Bruker µCT, Kontich, Belgium). For each µCT analysis, one grain was mounted with germ facing up and brush facing down on an appropriate sample holder. The µCT analysis were performed at two pixel sizes (pixel size = 1 µm or 7 µm).

At 7 µm pixel size, a 0.25 mm thick aluminum filter was employed together with an applied X-ray tube voltage of 26 kV and a source current of 197 µA. A camera with a resolution of 2016 x 1344 pixels was used. The scan orbit was 180° with a rotation step of 0.5°. Two images (2.9 sec of exposure time for each image) were taken per angular position and then averaged. A total of 385 projection images in TIFF format (16 bits) was obtained in approximatively 1 h for each grain. 30 grains of each selected wheat sample were scanned at 7 µm pixel size.

At 1 µm pixel size, a 0.25 mm thick aluminum filter was ~~is~~ employed together with an applied X-ray tube voltage of 31 kV and a source current of 216 µA. A camera with resolution of 2688 x 4032 pixels was used. The scan orbit was 180° with a rotation step of 0.1°. Two images (8 sec of exposure time for each image) were taken per angular position and averaged. The length of the grain was too important to be scanned in one run. The grain was scanned as 4 superimposed layers along the length of the grain to obtain the building of the entire 3D volume. The scan duration was about 54h and generated 7500 images in TIFF format (16 bits). Because of the scan duration (about 54h) and images analysis, three durum wheat grains were characterized at 1 µm pixel size. In order to assess as much as possible representative vitreous or porous structures of durum wheat endosperm, durum wheat grains containing both structures in well separated areas of the endosperm were selected (after visual inspection by transparency). Our experimental approach allowed the identification of the main µCT characteristics of the different structures in durum wheat endosperm. We did not describe the variability of the µCT parameters due to the diversity among grains.

2.3. Image reconstruction procedure

The batch of projection images was reconstructed with a modified Feldkamp algorithm (Feldkamp et al., 1984) using the SkyScanTM NRecon software (version 1.7.1.0) accelerated by GPU (Yan et al., 2008). Gaussian smoothing, misalignment correction, ring artefact reduction and beam hardening correction were applied.

For scans at 7 µm pixel size, post-alignment was specific for each grain. Smoothing, beam hardening and ring artifact correction parameters were similar for all grains and set to 1, 30%, 15 respectively according to the SkyScanTM NRecon software settings. The total reconstruction time was 40 sec for 1200 final cross-sectional images of 732 x 732 pixels.

For scans at 1 µm pixel size, 4 connected reconstruction scans were merged to form one scan length of 8060 images in cross-sectional plan. Misalignment correction was specific for each connected scan. Smoothing, beam hardening and ring artifact correction parameters were equivalent for each connected scan and set to 1, 30%, 10 respectively according to the SkyScanTM NRecon software settings. The total reconstruction time was about 2h for 8060 final cross-sectional images of 3912 x 3912 pixels.

2.4. Image processing and analysis

2.4.1. Volume of interest (VOI) determination

The reconstructed cross-sectional images were handled with CT Analyzer software (version 1.17.7.2) for 3D visualization of the scanned object and complete 3D quantitative analysis of the reconstructed volumes. The image processing steps included extraction of the volume of interest, segmentation, and calculation of morphometric parameters. The volume of interest was determined after a manual thresholding of the original image to obtain a binarized image and using a task list of several operations (despeckle, erosion and dilation).

At 7 µm pixel size, image processing was performed for the total volume of the grain. At 1 µm pixel size, image processing was performed for different VOI to focus specifically on dense or porous structures. Image processing was not possible for the total volume of the grain due to the image size (125 GigaOctet). To overcome this issue, 3 sets of 1300 cross-sectional images located at different positions along the z-axis of the grain, including dense and porous structure, were studied (*i.e.* slices).

2.4.2. Image analysis

3D morphometric parameters were extracted from each previously described VOI after image segmentation to binary using Otsu automatic method. Morphometric parameters were: volume of interest (mm^3), overall porosity (%), pore diameter distribution (µm). These parameters were based on analysis of a Marching Cubes (Lorensen and Cline, 1987) model with a rendered surface. 3D pore diameter was calculated using the “sphere-fitting” (double distance transform) method (Borgefors, 1996; Remy and Thiel, 2002). The overall porosity was calculated by the ratio of air volume over the total volume of interest. The pores were described by pore diameter values. The pore-size distribution curves were expressed by the volume ratio abundance of each pore size in the total volume of pore. The pore median diameter (D_{50}) corresponded to the pore diameter of 50% of the pore population. The absolute span value of pore-size diameter was (D_{90}-D_{10}).

2.4.3 Volume rendering

Surface-rendered 3D models were constructed for 3D viewing of the grain analyzed regions, using SkyScan CTVolume ("CTVox") software. Model construction was carried out with the "Double time cubes" method (Bouvier, 2004), which is a modification of the Marching cubes method (Lorensen and Cline, 1987).

2.5. Statistical analysis

The statistical analysis was performed using R software and Rstudio software (version 1.2.5033). Analysis of variance by Tukey multiple comparison range test were conducted at 5% significant level.

3. Results and discussion

3.1. µCT analysis at 7 µm pixel size

Endosperm of durum wheat grains was studied by µCT at 7 µm pixel size in order to classify grains according to their porosity. The experiments were conducted on the two selected wheat samples.

3.1.1. µCT image reconstruction of the total durum wheat grain

Fig. 1A gives an example of one projection image (scanned at 7 µm pixel size) of a durum wheat grain, among the 385 collected images for each grain. The projection images are 2-dimensional radiograph, with a greyscale shade depending on the density.

The batch of 385 projection images were consolidated to reconstruct 1200 cross-sectional images for each grain, and one 3D image of the whole grain volume. One example of cross-sectional image of durum wheat grain is presented in **Fig. 1B**. We observe an apparent uniform grey color for the internal endosperm, with few differences in grey density. The peripheral aleurone layer is clearly visible in brighter grey. Porosity between the aleurone layer and the envelopes appears in black. For each of the 1200 cross-sectional images, the region of interest was defined without the envelopes. This makes it possible to remove the porosity at the envelopes-aleurone interface and the porosity of the crease from the analysis (**Fig. 1C**). The white area of the region of interest was considered for µCT image processing. The volume of interest corresponded to the stack of regions of interest designed on each cross-sectional image. With the Otsu thresholding method, white and black pixels corresponded to dense and porous structure respectively. At 7 µm pixel size acquisition, the endosperm is thus mostly describe as a dense structure (**Fig. 1D**).

3.1.2. µCT morphometric parameters determination

We calculated an overall porosity for each of the 30 grains of the wheat samples (**Fig. 2A**). Large differences were observed among the minimum (0.049%) and maximum (0.185%) values of porosity between grains. To evaluate data dispersion, the mean and standard deviation values of porosity were calculated as a function of the number of grains considered (from 2 to 30 grains), for the 2 wheat samples (**Fig. 2A**). When less than 10 grains were considered, differences between grains induce large fluctuations in mean and standard deviations values. When considering 10-20 grains, the mean and standard deviation values converge towards a constant value. About 25 grains were enough to stabilize the mean and standard deviation values of the overall porosity of grains. The calculations were made with 30 grains of each wheat sample. The overall porosity of the Pescadou wheat variety (0.100 ± 0.041) was not significantly different from that of the Karur wheat variety (0.104 ± 0.035). µCT at 7 µm pixel size from 30 grains did not allow to significantly discriminate the porosity of the 2 wheat samples.

Analysis of µCT images scanned at 7 µm for each grain was considered by constructing the cumulative distribution curves of the pore volume, as a function of the apparent pores diameter. The description of the 60 distribution curves constructed for each selected durum wheat grain (data not shown) allowed the identification of three specific patterns (**Fig. 2B**), which were associated with three different porosity types in the endosperm. The curves could display a monomodal pattern, with a single type of pores of similar diameter (D_{50} = 7-9 µm) or a bimodal pattern having 2 pore populations of small (D_{50} = 7-9 µm) or intermediate (D_{50} = 45-60 µm) diameters. They could also display a multimodal pattern having at least 3 pore populations: small (D_{50} = 7-9 µm), intermediate (D_{50} = 45-65 µm), or large (D_{50} = 90-120 µm) diameters. Value proximity between D_{50} of the smaller population (D_{50} = 7-9 µm) and the pixel size (7 µm) implies that noise is probably included in the analysis. Nevertheless, as this is a comparative analysis and as the pre-processing is identical for image batches, this artifact can be overlooked. In order to reach more accurate pore size values, it will be necessary to explore a pixel size smaller than the one of the smallest pores.

Analysis of µCT images scanned at 7 µm allowed thus the identification of three pore populations in durum wheat endosperms. Each grain can be classified according to one of these patterns (**Table 1**).

For each grain and population of pores, we calculated the pore median diameter (D_{50}) and their relative proportion (**Table 1**). Each grain can be classified according to ~~in~~ one of the three categories related to porosity distribution:

- Grain with endosperm containing 100% of small pores (7-9 µm).
- Grain with endosperm containing 88-92% of small pores (7-9 µm) and 7-12% of intermediate pores (45-60 µm).
- Grain with endosperm containing 72-76% of small pores (7-9 µm), 15-18% of intermediate pores (45-65 µm) and 6-14% of large pores (100-120 µm).

Analysis of µCT images scanned at 7 µm pixel size made it possible to classify the durum wheat grains based on the distribution of pore characteristics.
Grains of the Pescadou sample (0% porous) were found to present a dense endosperm without any porosity according to the reference method (Pohl grain cutter). By considering µCT results, they were classified as having a large proportion of grains (63%) with small pores, a medium proportion (30%) with intermediate pores, and a small proportion (7%) with large pores. A major part of the grains (93 %) only contained small or intermediate pores. These pores could be associated to small irregularities (e.g. large fractures) in the endosperm, which are not considered as "mealy" structure according to the reference method. Analysis of µCT images scanned at 7 µm pixel size allowed to identify a low proportion of grains (7%) with large pores. However, it only represented 2 grains in the sample.

Grains of the Karur wheat sample were characterized by the presence of 33% of porous grains according to the reference method. By considering µCT results, they were classified as having a low proportion of grains (17%) with small pores, a large proportion (50%) with intermediate pores, and a large proportion (33%) with large pores. This value was similar to the proportion of porous grains for the Karur variety as measured by the reference method. The large pores could be associated to porous areas in the endosperm, which were considered as "mealy" structures according to the reference method. µCT analysis at 7 µm pixel size could then be considered for ~~to~~ the classification of porous grains distributions in a batch of durum wheat grains.

3.2. µCT analysis at 1 µm pixel size

The endosperm structures of three durum wheat grain (Karur sample) were studied by µCT at 1 µm pixel size in order to define criteria describing the microstructure of dense (*i.e.* vitreous) and porous (*i.e.* mealy) structures.

3.2.1. Cross-sectional images reconstruction

At 1 µm pixel size, the acquisition of a grain had to be carried out in 4 successive scans performed along the length of the grain. The projection 2D images displayed slight differences in the grey. The crease and the germ appeared in a lighter shade of grey, as an area of lower density.

The batch of projection images were consolidated to reconstruct cross-sectional images of the grain and one 3D image of the whole wheat grain volume. The use of image-processing software made it possible to use the cross-sectional images in order to view the 3D representation of the durum wheat grain.

One example of µCT cross-sectional image of durum wheat endosperm obtained after reconstruction is presented in **Fig. 1SA** (supplementary material). The porous structures were dark grey. The dense structures were light grey. The aleurone layer and the envelopes surrounding the starchy endosperm were clearly visible. For the construction of the regions of interest, the envelopes were not taken into account nor the porosity at the envelopes-aleurone layer interface nor the porosity of the crease (**Fig. 1SB and 1SC**, supplementary material). The image inside the cross-sectional region of interest with different shades of grey was segmented into a binary image using Otsu automatic method (**Fig. 1SD**, supplementary material). We could note that some ring artefacts were still included as background after binarization.

3.2.2 Images processing methodology

An original method of image processing was developed to separately analyze the porous and the dense structures within the endosperm. Each cross-sectional image in the region of interest was separated in 2 regions of interest (**Fig. 3A**), by differentiating the porous and the dense structure. The grey-scale image in the cross-sectional region of interest with different shades of grey **(Fig. 3B)** was segmented into a binary image using Otsu automatic method **(Fig. 3C)**. Regions of interest were first designed for the porous structure. Despeckle step and morphological operation (erosion, dilatation tool) were used as cleaning parameters on cross-sectional images manually thresholded. Processing was completed by image bitwise operations in order to easily isolate the volume of interest of the porous structure. Then, regions of interest of the dense structure were designed by subtracting the region of interest of the porous structure from that of the endosperm's total region.

Due to the large number of cross-sectional images and the limited capacity of the computer, we were not able to construct a single 3D data set in order to describe the total volume of the wheat grain. We selected three sets of 1300 cross-sectional images, corresponding to three 3D slices of 1.3 mm thickness along the length of the grain, and located in the central part of the grain. The germ and the brush part were not considered. Image processing and morphometric parameters calculation were performed on these three 3D slices, corresponding to the volumes of interest of the structures.

3.2.3. μCT morphometric parameters determination

The calculated values of volumes of interest provide access to the respective volumes of dense and porous structures in each 3D slice of the grain. The porosity of each 3D slice was also calculated (**Table 2**). We constructed the cumulative distribution curves of pore volume as a function of the apparent pores diameter (**Fig. 4**). The characteristic parameters (D_{50} ; span ; % pore volume) of the cumulative distribution curves are presented in **Tables 2**.

Porous structures of the endosperm were characterized by high porosity (27.9% ±1.7) (**Table 2**). The volume of interest of porous structure (3.35 mm^3) corresponded approximately to 41% of the total endosperm volume of the 3 grains. The cumulative distribution curves of pore volume as a function of pore diameter displayed a monomodal pattern, with a single type of porosity (**Fig. 4**). Porosity was characterized by a median diameter (D_{50}) of 3.42 (± 0.25) µm with large dispersion (span = 6.7 µm) (**Table 2**). The porous structures contained a single type of pores.

The volume of the dense structures (4.69 mm^3) corresponded approximately to 58% of the total volume of the endosperm (**Table 2**). The µCT analysis at 1 µm pixel size indicated the presence of porosity in the dense structures of the endosperm, with 8.8% (±3.0) of porosity. In dense structure, the cumulative distribution curves of pore volume as a function of pore diameter displayed a bimodal pattern, with two types of porosity (**Fig. 4**). The main pores (72% of the pore volume) were characterized by low diameter (1.39 µm) and low dispersion (span = 3.0 µm) (**Table 2**). The second minor population of pores (28% of the pore volume) were characterized by a higher diameter (9.2 µm) and a high dispersion (10.4 µm). The dense structures were poorly porous. Their low porosity was due to the presence of a large number of very small pores, and few large pores.

Almost similar porosity values were measured for common wheat grains endosperm (3-13%) and hard wheat grains endosperm (2-8%) (Dobraszczyk et al., 2002; Schoeman et al., 2016). Pore diameters between 1 and 8 µm were measured with mercury intrusion porosimeter in endosperm of different common wheat grains (Greffeuille et al., 2007). Our results consolidate the fact that the open structure of mealy durum wheat endosperm is contrasted with the compact structure of vitreous durum wheat endosperm (Dexter et al., 1989). Vitreous endosperms had higher density than mealy endosperms, due to the absence of air spaces. Samson et al. (2005) calculated the entrapped air volume in endosperm of durum wheat grains by performing density measurements. The estimated air volumes widely differed between vitreous (0.2-2.8%) and mealy (7.0-12.4%) endosperms in durum wheat grain. Entrapped air volume was at least 6 times greater for mealy endosperm.

As expected, the calculated porosity of the grain slices (15.8% ±5.7) was intermediate between the porosity of the dense (9%) and the porous (28%) structures (**Table 2**). Porosity depended on the proportion of porous and dense structures in the durum wheat grain endosperm. High values of standard deviation can highlight differences of vitreousness between different slices. In grain slices, the cumulative distribution curves of pore volume as a function of pore diameter displayed a monomodal pattern, with a single type of porosity (**Fig. 4**). Porosity was due to the presence of pores with low diameter (2.91 ± 0.39 µm) with a large dispersion of values (span = 6.3 µm) (**Table 2**), close to those previously observed for the porous structures. In the grain slices, we were not able to identify the presence of very small and large pores, as previously observed in the dense structures (**Fig. 4**). The number of large pores could be very low and not detectable on the cumulative distribution curves. µCT analysis at 1 µm pixel size improved thus the description of the structure characteristics of durum wheat endosperm, by considering the cumulative distribution curve of pore volume as a function of pore diameter.

4. Conclusion

µCT methods are interesting tools for characterizing the structure of durum wheat endosperm and generating useful information depending on the pixel size (1 or 7 µm) used for image scanning.

The µCT analysis at 7 µm pixel size made it possible to discriminate by statistical approach two wheat grain samples according to their porosity characteristics. µCT data were analyzed by constructing the cumulative distribution curves of pore volume as a function of pore diameter. The analysis of the different type of pores was used to describe the endosperm structure and could be related to grain vitreousness. µCT analysis at 7 µm considered the structural characteristics of the entire volume of the endosperm. However, the µCT analysis at 7 µm pixel size of one grain took about 1 hour. This method could not be considered as a rapid method to classify batches of durum wheat grains, but can be used to investigate grain structure and compare grains using a qualitative approach.

µCT analysis at 1 µm pixel size determined parameters that could be used to describe the endosperm microstructure of durum wheat grain and quantified the proportion of mealy and vitreous endosperm. Porosity characteristics can be used to differentiate and describe both the dense and porous structures. The µCT analysis at 1 µm pixel size can be considered to improve the description of the micro-structure of durum wheat endosperm. However, the time required to scan µCT images at 1 µm pixel size with laboratory equipment appears too long (about 54 hours). In addition, the very large number of scans led to tedious analysis. The µCT method could still be further explored with different durum wheat grains structures to consolidate the discussion on the pore diameter distribution in the endosperm.

ACKNOWLEDGEMENTS

This work was supported by BPI France through the research program “DEFI Blé Dur”. The authors acknowledge Arvalis (Institut du Végétal, France) for providing durum wheat grains, Léa Ollier (CIRAD, UMR Qualisud, France) for providing help during image processing and analysis, and Reine Barbar (INRAE, UMR IATE, France) for manuscript redaction.

REFERENCES

AFNOR, 2016. Produits alimentaires - Détermination de la teneur en azote total par combustion selon le principe Dumas et calcul de la teneur en protéines brutes - Partie 2 : céréales, légumineuses et produits céréaliers de mouture. Normes Françaises V03-767–2.

AFNOR, 2014. Blé dur (Triticum durum Desf.) - Détermination du taux de mitadinage - Méthode avec un appareil de coupe. Normes Françaises V03-779.

AFNOR, 2010. Céréales et produits céréaliers - Détermination de la teneur en eau - Méthode de référence. Normes Françaises V03-707.

Borgefors, G., 1996. On digital distance transforms in three dimensions. Computer Vision and Image Understanding. 64, 368–376. https://doi.org/10.1006/cviu.1996.0065

Bouvier, D.J., 2004. Double-time cubes: a fast 3D surface construction algorithm for volume visualisation University of Arkansas, 313 Engineering Hall, Fayetteville, AR72701, USA.

Chichti, E., Carrère, M., George, M., Delenne, J.Y., Lullien-Pellerin, V., 2018. A wheat grain quantitative evaluation of vitreousness by light transmission analysis. Journal of Cereal Science. 83, 58–62. https://doi.org/10.1016/j.jcs.2018.07.009

Dexter, J.E., Marchylo, B.A., MacGregor, A.W., Tkachuk, R., 1989. The structure and protein composition of vitreous, piebald and starchy durum wheat kernels. Journal of Cereal Science. 10, 19–

32. https://doi.org/10.1016/S0733-5210(89)80031-1

Dobraszczyk, B.J., Whitworth, M.B., Vincent, J.F.V., Khan, A.A., 2002. Single kernel wheat hardness and fracture properties in relation to density and the modelling of fracture in wheat endosperm. Journal of Cereal Science. 35, 245–263. https://doi.org/10.1006/jcrs.2001.0399

Edwards, N.M., Zhang, N., Dowell, F.E., Pearson, T., 2005. Determining vitreousness of durum wheat using transmitted and reflected images. Transactions of the ASAE. 48, 219–222. https://doi.org/10.13031/2013.17920

Feldkamp, L.A., Davis, L.C., Kress, J.W., 1984. Practical cone-beam algorithm. Journal of the Optical Society of America. 1, 612-619. https://doi.org/10.1364/JOSAA.1.000612

Fu, B.X., Wang, K., Dupuis, B., Taylor, D., Nam, S., 2018. Kernel vitreousness and protein content: Relationship, interaction and synergistic effects on durum wheat quality. Journal of Cereal Science. 79, 210–217. https://doi.org/10.1016/j.jcs.2017.09.003

Greffeuille, V., Abecassis, J., Barouh, N., Villeneuve, P., Mabille, F., Bar L'Helgouac'h, C., Lullien-Pellerin, V., 2007. Analysis of the milling reduction of bread wheat farina: Physical and biochemical characterisation. Journal of Cereal Science. 45, 97–105. https://doi.org/10.1016/j.jcs.2006.07.003

ICC, 1986. Recommendation No. 202: Procedure for near infrared (NIR) reflectance analysis of ground wheat and milled wheat products. International Association for Cereal Science and Technology. Vienna, Austria.

Kaya, E., Saritas, İ., 2019. Towards a real-time sorting system: Identification of vitreous durum wheat kernels using ANN based on their morphological, colour, wavelet and gaborlet features. Computers and Electronics in Agriculture. 166, 105016. https://doi.org/10.1016/j.compag.2019.105016

Le, T.D.Q., Alvarado, C., Girousse, C., Legland, D., Chateigner-Boutin, A.L., 2019. Use of X-ray micro computed tomography imaging to analyze the morphology of wheat grain through its development. Plant Methods. 15, 1–19. https://doi.org/10.1186/s13007-019-0468-y

Lorensen, W.E., Cline, H.E., 1987. Marching cubes: A high resolution 3D surface construction algorithm, in: Proceedings of the 14th Annual Conference on Computer Graphics and Interactive Techniques - SIGGRAPH '87. Presented at the 14th annual conference, ACM Press, pp. 163–169. https://doi.org/10.1145/37401.37422

Neethirajan, S., Jayas, D.S., White, N.D.G., 2007. Detection of sprouted wheat kernels using soft X-ray image analysis. Journal of Food Engineering. 81, 509–513. https://doi.org/10.1016/j.jfoodeng.2006.11.020

Neethirajan, S., Karunakaran, C., Symons, S., Jayas, D.S., 2006. Classification of vitreousness in durum wheat using soft X-rays and transmitted light images. Computers and Electronics in Agriculture. 53, 71–78. https://doi.org/10.1016/j.compag.2006.03.001

Raggiri, V., Abecassis, J., Mabille, F., Samson, M.F., Barron, C., Lullien-Pellerin, V., 2014. Compréhension et détermination des facteurs clés de la valeur semoulière. Industries des Céréales. 189, 11–21.

Remy, E., Thiel, E., 2002. Medial axis for chamfer distances: computing look-up tables and neighbourhoods in 2D or 3D. Pattern Recognition Letters. 23, 649–661. https://doi.org/10.1016/S0167-8655(01)00141-6

Samson, M.F., Mabille, F., Chéret, R., Abecassis, J., Morel, M.H., 2005. Mechanical and physicochemical characterization of vitreous and mealy durum wheat endosperm. Cereal Chemistry. 82, 81–87. https://doi.org/10.1094/CC-82-0081

Schoeman, L., du Plessis, A., Manley, M., 2016. Non-destructive characterisation and quantification of the effect of conventional oven and forced convection continuous tumble (FCCT) roasting on the three-dimensional microstructure of whole wheat kernels using X-ray micro-computed tomography (μCT). Journal of Food Engineering. 187, 1–13. https://doi.org/10.1016/j.jfoodeng.2016.04.015

Sissons, M., Abecassis, J., Marchylo, B., Cubadda, R., 2012. CHAPTER 12 - Methods used to assess and predict quality of durum wheat, semolina, and pasta, in: Sissons, M., Abecassis, J., Marchylo, B., Carcea, M. (Eds.), Durum Wheat (Second Edition), American Associate of Cereal Chemists International. AACC International Press, pp. 213–234. https://doi.org/10.1016/B978-1-891127-65-6.50017-9

Sissons, M.J., Osborne, B.G., Hare, R.A., Sissons, S.A., Jackson, R., 2000. Application of the Single-Kernel Characterization System to durum wheat testing and quality prediction. Cereal Chemistry. 77, 4–10. https://doi.org/10.1094/CCHEM.2000.77.1.4

Strange, H., Zwiggelaar, R., Sturrock, C., Mooney, S.J., Doonan, J.H., 2015. Automatic estimation of wheat grain morphometry from computed tomography data. Functional Plant Biology. 42, 452. https://doi.org/10.1071/FP14068

Suresh, A., Neethirajan, S., 2015. Real-time 3D visualization and quantitative analysis of internal structure of wheat kernels. Journal of Cereal Science. 63, 81–87. https://doi.org/10.1016/j.jcs.2015.03.006

Venora, G., Grillo, O., Saccone, R., 2009. Quality assessment of durum wheat storage centres in Sicily: Evaluation of vitreous, starchy and shrunken kernels using an image analysis system. Journal of Cereal Science. 49, 429–440. https://doi.org/10.1016/j.jcs.2008.12.006

Vermeulen, P., Suman, M., Fernández Pierna, J.A., Baeten, V., 2018. Discrimination between durum and common wheat kernels using near infrared hyperspectral imaging. Journal of Cereal Science. 84, 74–82. https://doi.org/10.1016/j.jcs.2018.10.001

Yan, G., Tian, J., Zhu, S., Dai, Y., Qin, C., 2008. Fast cone-beam CT image reconstruction using GPU hardware. Journal of X-Ray Science and Technology. 16, 225–234.

Zhu, L.J., Dogan, H., Gajula, H., Gu, M.H., Liu, Q.Q., Shi, Y.C., 2012. Study of kernel structure of high-amylose and wild-type rice by X-ray microtomography and SEM. Journal of Cereal Science. 55, 1–5. https://doi.org/10.1016/j.jcs.2011.08.013

FIGURE CAPTIONS

Fig. 1. µCT cross-sectional images at 7 µm pixel size of one durum wheat grain (Karur sample). µCT projection image (A); grey-scale image (B); image of the region of interest (C); image after Otsu thresholding method (D).

Fig. 2. Overall porosity (%) of durum wheat grains as a function of the number of grains scanned (A) and typical cumulative distribution curves of pore volume as a function of apparent pores diameter for three durum wheat grains (B) determined from µCT analysis at 7 µm pixel size.

Fig. 3. µCT cross-sectional images at 1 µm pixel size for the porous (left) and dense structure (right) of the endosperm (Karur sample). Image of the region of interest (A) ; grey-scale image in the region of interest (B) ; image after Otsu thresholding method (C).

Fig. 4. Typical cumulative distribution curves of pore volume as a function of apparent pores diameter in durum wheat endosperm (for 1 slice) determined from µCT analysis at 1 µm pixel size: porous structures (○), dense structures (●) and endosperm (●).

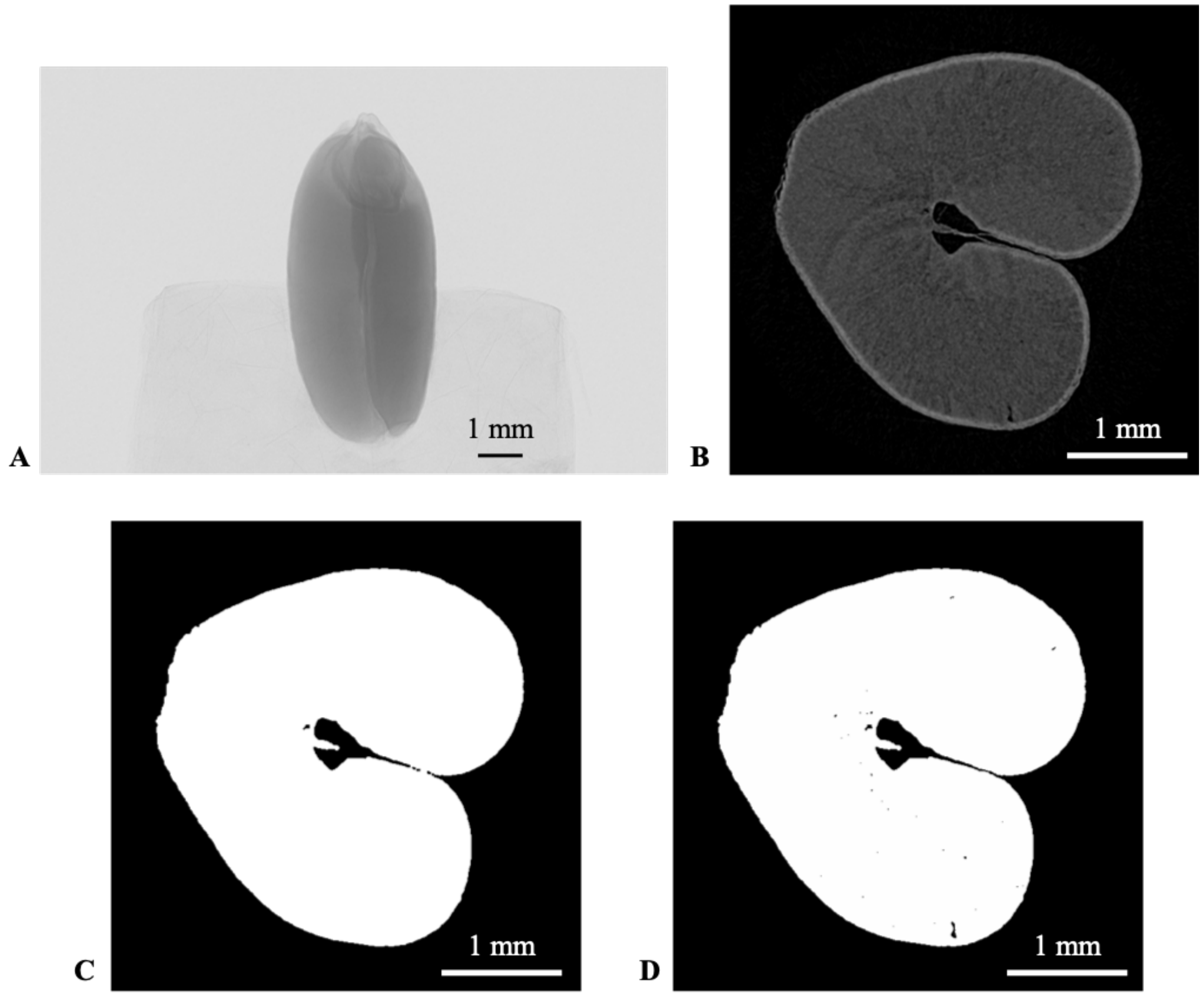

Fig. 1. μCT cross-sectional images at 7 μm pixel size of one durum wheat grain (Karur sample). μCT projection image (A); grey-scale image (B); image of the region of interest (C); image after Otsu thresholding method (D).

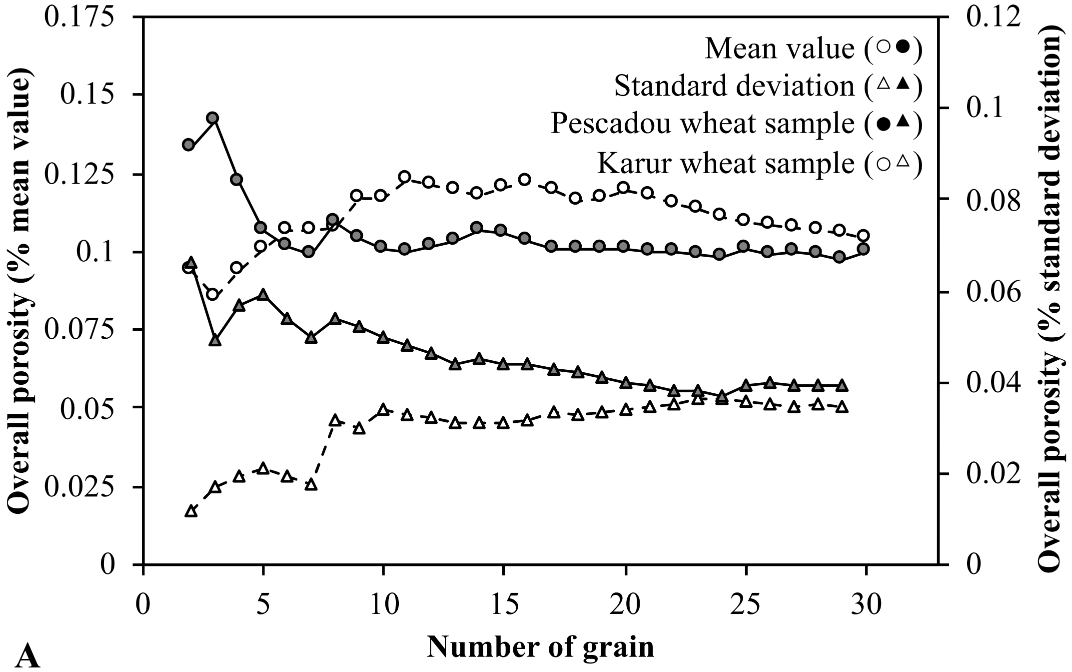

A

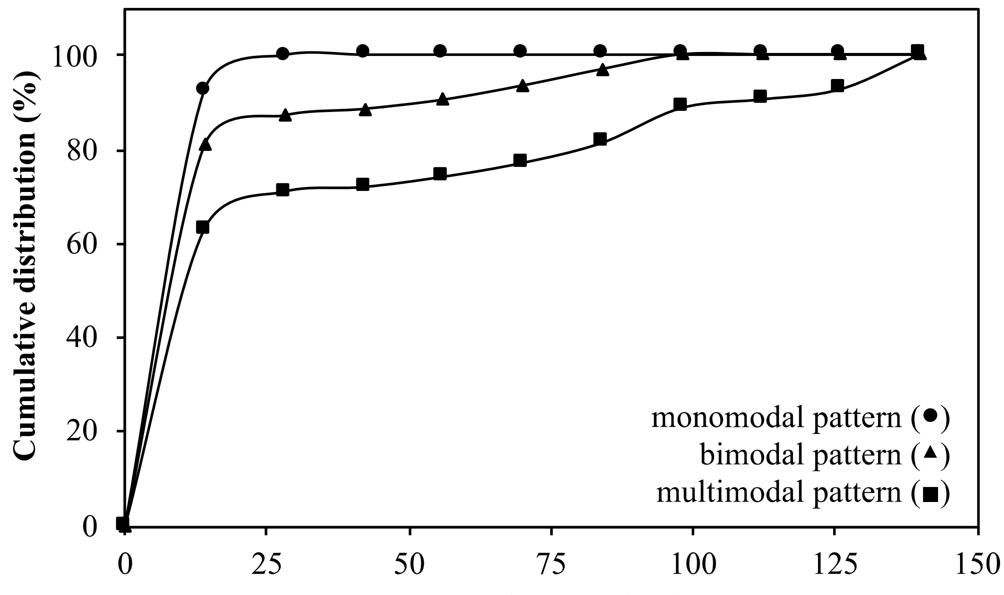

B

Fig. 2. Overall porosity (%) of durum wheat grains as a function of the number of grains scanned (A) and typical cumulative distribution curves of pore volume as a function of apparent pores diameter for three durum wheat grains (B) determined from µCT analysis at 7 µm pixel size.

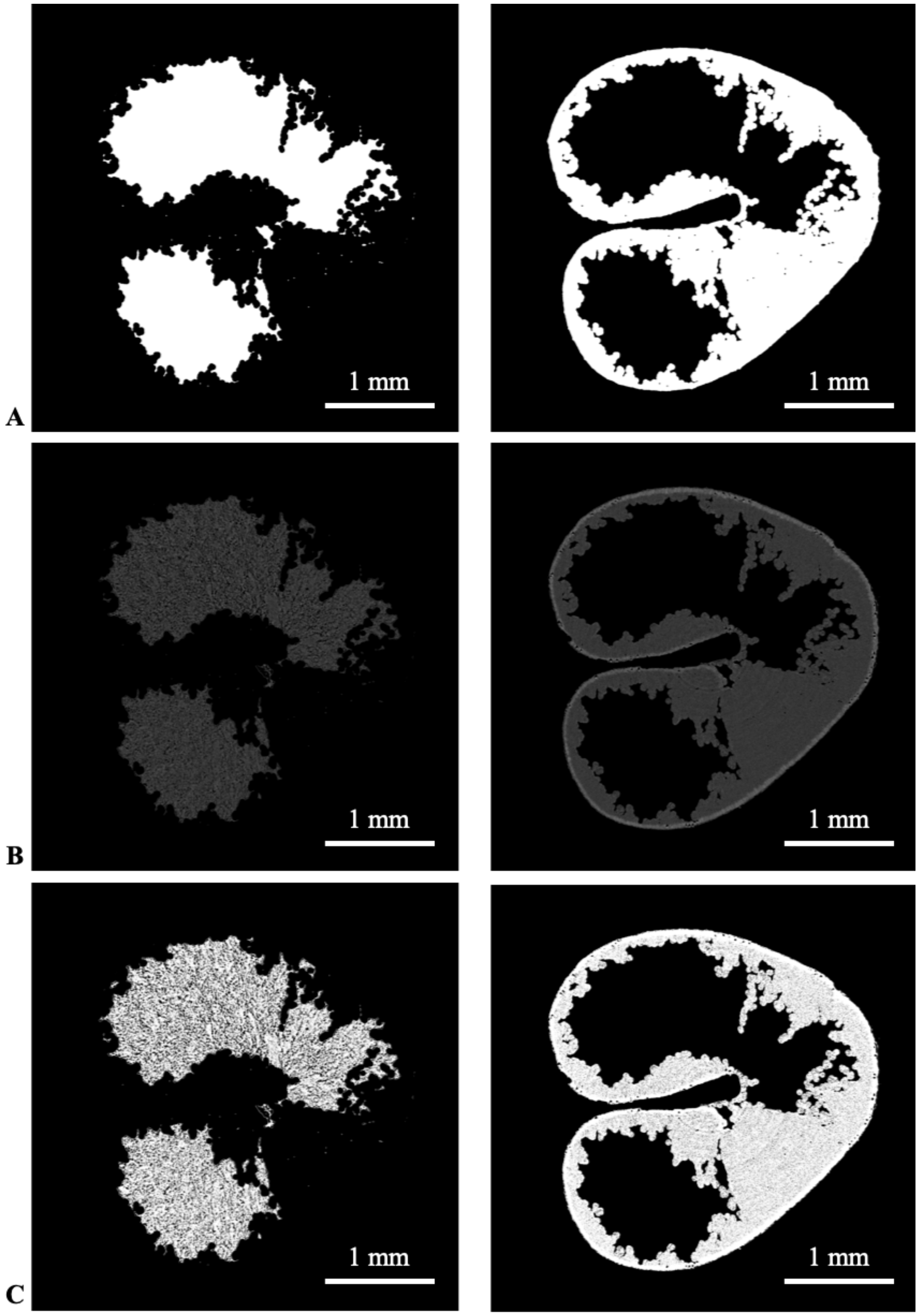

Fig. 3. μCT cross-sectional images at 1 μm pixel size for the porous (left) and dense structure (right) of the endosperm (Karur sample). Image of the region of interest (A) ; grey-scale image in the region of interest (B) ; image after Otsu thresholding method (C).

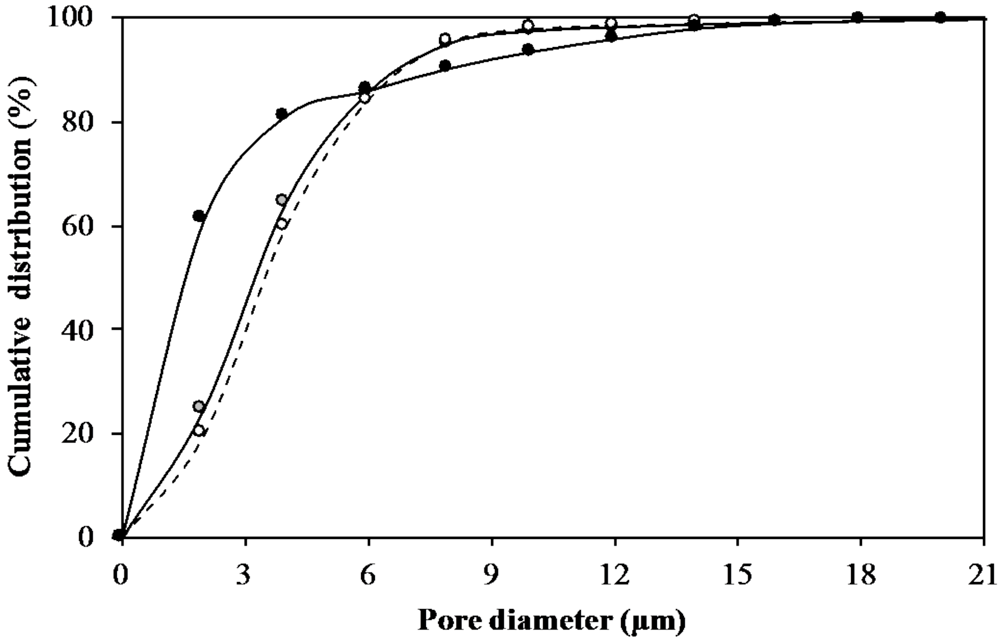

Fig. 4. Typical cumulative distribution curves of pore volume as a function of apparent pores diameter in durum wheat endosperm (for 1 slice) determined from µCT analysis at 1 µm pixel size: porous structures (○), dense structures (●) and endosperm (●).

TABLES

Table 1. Morphometric parameters (D_{50}) associated to the cumulative distribution curves of pore volume as a function of apparent pores diameter (monomodal, bimodal or multimodal pattern) for the grains of the two selected wheat varieties, determined from µCT images scanned at 7 µm resolution.

	Small pores		Intermediate pores		Large pores	
	Proportion ***(%)***	**D_{50}** ***(µm)***	**Proportion** ***(%)***	**D_{50}** ***(µm)***	**Proportion** ***(%)***	**D_{50}** ***(µm)***
Pescadou wheat sample (n = 30)						
One type of pores (n = 19)	100	7.63 (±0.36) [a]	--	--	--	--
Two types of pores (n = 9)	88.0 (±6.7)	7.28 (±0.79) [a]	12.0 (±6.7)	60.4 (±8.1) [a]	--	--
Three types of pores (n = 2)	76.1 (±7.2)	7.90 (±0.02) [ab]	18.0 (±2.7)	63.7 (±26.0) [a]	6.35 (±4,5)	108 (±31.2) [a]
Karur wheat sample (n = 30)						
One type of pores (n = 5)	100	8.86 (±1.08) [b]	--	--	--	--
Two types of pores (n = 15)	92.8 (±7.5)	7.96 (±0.61) [ab]	7.2 (±7.5)	57.1 (±12.2) [a]	--	--
Three types of pores (n = 10)	71.8 (±7.2)	7.80 (±0.63) [ab]	14.6 (±6.7)	54.3 (±8.8) [a]	13.7 (±3.9)	92.4 (±14.5) [a]
Overall wheat grains	--	7.80 (±0.71) [a]	--	57.5 (±11.0) [a]	--	94.7 (±16.2) [a]

Note : Results are presented as mean ± standard deviation from the values obtained for the 30 grains of each variety. The presence of common letters in the same column indicate no significant difference (P_{value} > 0,05).

Table 2. Morphometric parameters of endosperm of durum wheat grain (porosity and volume of interest), and morphometric parameters (D_{50} and Span) associated to the cumulative distribution curves of pore volume as a function of apparent pores diameter, determined from µCT images scanned at 1 µm.

	Porosity *(%)*	**Volume of interest** *(mm^3)*	**D_{50}** *(µm)*	**Span** *(µm)*	**% pore volume** *(%)*
Porous part of the grain slices	27.9 (±1.7) [a]	3.35 (±1.93) [a]	3.42 (±0.25) [b]	6.73 (±1.98)	100%
Dense part of the grain slices	8.8 (±3.0) [c]	4.69 (±1.22) [a]	1.39 (±0.05) [a]	3.00 (±0.06)	72%
			9.24 (±1.59) [c]	10.44 (±1.38)	28%
Grain slices	15.8 (±5.7) [b]	--	2.91 (±0.39) [b]	6.32 (±1.38)	100%

Note : Results are presented as mean ± standard deviation from the values obtained for the nine 3D slices from three durum wheat grains. The presence of common letters in the same column indicate no significant difference (P_{value} > 0,05). With Span = D_{90} - D_{10}.

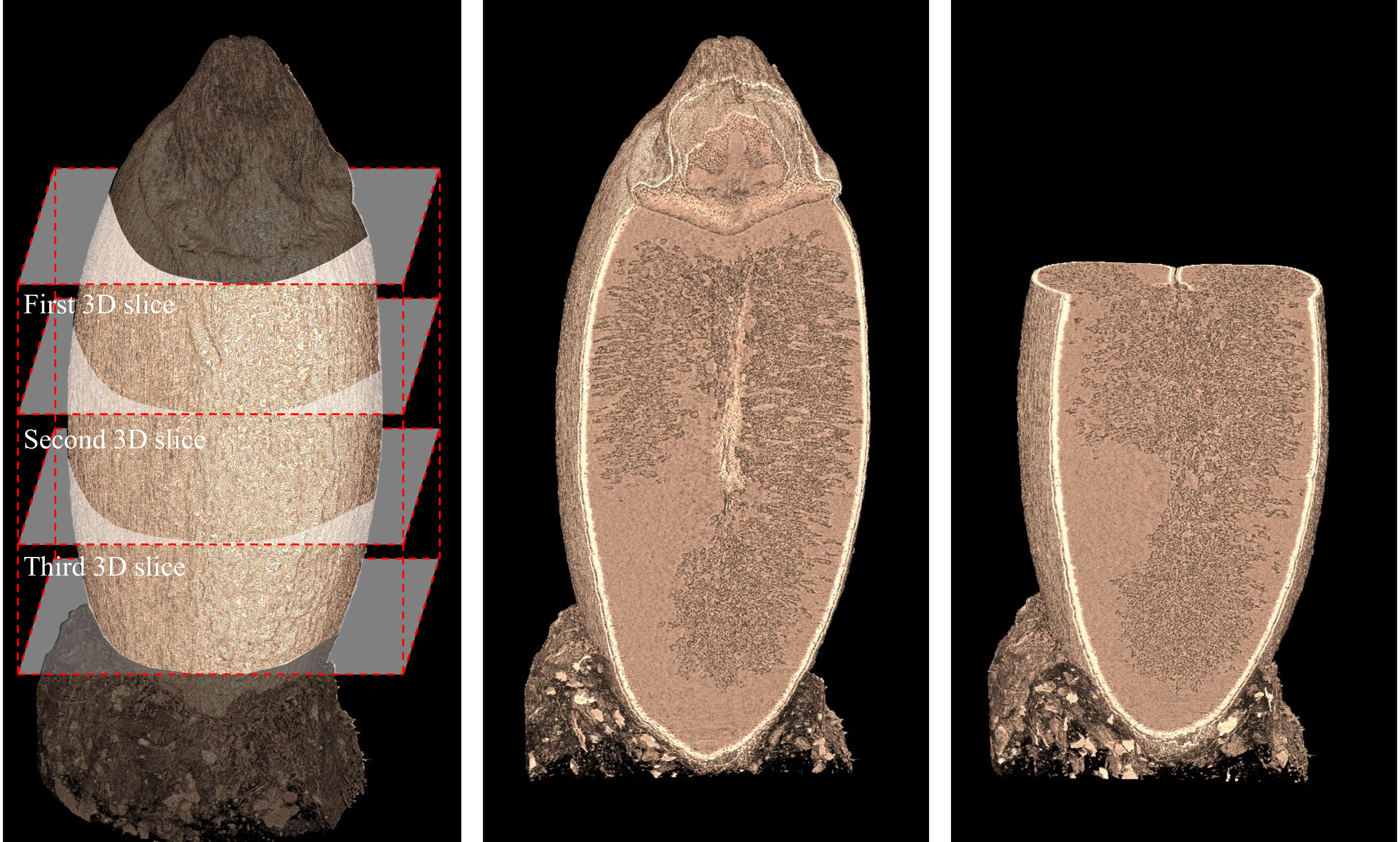
First 3D slice
Second 3D slice
Third 3D slice